Journal of Saudi Chemical Society (2015) xxx, xxx–xxx

King Saud University

Journal of Saudi Chemical Society

www.ksu.edu.sa
www.sciencedirect.com

ORIGINAL ARTICLE

Surfactant free fabrication of copper sulphide (CuS–Cu_2S) nanoparticles from single source precursor for photocatalytic applications

Umair Shamraiz [a], Amin Badshah [a,*], Raja Azadar Hussain [a], Muhammad Amtiaz Nadeem [b], Sonia Saba [c]

[a] *Department of Chemistry, Quaid-i-Azam University, Islamabad 45320, Pakistan*
[b] *Department of Environmental Sciences, Quaid-i-Azam University, Islamabad 45320, Pakistan*
[c] *PIASA NARC, Islamabad 45320, Pakistan*

Received 30 April 2015; revised 12 July 2015; accepted 14 July 2015

KEYWORDS

Chalcogenides;
Photo catalysts;
Dye degradation

Abstract A simple, ethylene glycol chemical reduction method was employed to synthesize CuS–Cu_2S nanoparticles from single source copper thiourea complex for removal of persistent organic dyes. Fabricated CuS–Cu_2S nanoparticles were characterized by powder XRD (PXRD), energy dispersive X-ray spectroscopy (EDX), selected area electron diffraction (SAED), transmission electron microscopy (TEM) and high resolution transmission electron microscopy (HRTEM). Photocatalytic behaviour of CuS–Cu_2S nanoparticles was evaluated under direct sunlight for degradation of methylene blue, malachite green, methyl orange, methyl violet and rhodamine B with the help of UV–vis spectroscopy.

1. Introduction

Among metal chalcogenides copper sulphide nanoparticles have been extensively synthesized due to their potential applications as p-type semiconductors. Some critical parameters have been established over the years which are necessary to control morphology, because reaction can be induced by different parameters which are: reaction temperature, solvent used, concentration of precursors used, power and time of irradiation, complexing agent and pH of the solution [1]. In nature copper sulphide exists in different phases which can be easily synthesized by controlling molar ratios of copper and sulphur i.e. CuS (covellite) dispersed particles, Cu_7S_4–CuS hexagonal plates, Cu_9S_5 (Digenite) octahedron, and Cu_2S (chalcocite). In recent years CuS has been synthesized with different morphologies such as nanotubes [2], nanowires [3], nano plates [4], nano rods [5], ball-flower [6], nanoparticles [7], hollow cages [8] and hollow sphere [9] with biological sulphate

* Corresponding author. Tel.: +923009780374.
E-mail addresses: umairshamraiz@gmail.com (U. Shamraiz), aminbadshah@yahoo.com (A. Badshah), hussainazadar@yahoo.com (R.A. Hussain), manadeempk@gmail.com (M.A. Nadeem), Soniasaba88@yahoo.com (S. Saba).

Peer review under responsibility of King Saud University.

Production and hosting by Elsevier

http://dx.doi.org/10.1016/j.jscs.2015.07.005

reduction [10], chemical route [11], chemical vapour deposition [12], chemical vapour reaction (CVR) [13], hydrothermal method [3], electrospinning [14], sono-chemical method [15], solid state synthesis [16], liquid precipitation route [17], liquid–liquid interface [18], pressure leaching process [19], micro-emulsions [20] and self-sacrificial templates [21]. Covellite (CuS) proved to be a very fruitful nanomaterial for solar cell applications [22], photocatalytic degradation of dyes [23], as a cathode material in lithium ion rechargeable secondary batteries [24], gas sensing [25] etc. Cu_2S (chalcocite) possessing bulk band gap of 1.21 eV is a p-type semiconductor which lies in an optimum range for solar energy conversion [26], solar cells [27], catalysis [28], efficient photo catalyst [29], biosensors [30] and potential applications in optoelectronics devices [31]. Hence, efforts were made to find out new methods for the synthesis of Cu_2S nanostructures with different morphologies such as nanoparticles [32], nanowires [33], nano plates [27], dendrites [34] hollow microspheres [35] and mixed CuS–Cu_2S [36].

Nanomaterials proved to be environmentally friendly candidates for removing chemical wastes because they are easy to regenerate and are effective in dye removal from waste water. (CuS–Cu_7S_4) proved to be very fruitful for degradation of rhodamine B [37]. CuS–Cu_2S nanoparticles were successfully used to degrade methyl orange [38]. The photocatalytic activity of Cu_2S was evaluated against Active Brilliant Red X-3B, 11.7% for nanoparticles, 20.3% for nanowires and 50.1% for nano flowers [39]. CuS with different morphologies exhibits different band gaps and are being used by different research groups for degradation of organic dyes [29]. All of them use UV light or indoor lightening as a source of energy to create electron hole pair for dye degradation.

In our present research CuS–Cu_2S nanoparticles were fabricated through single source precursor for photocatalytic activity. It is a well established fact that reduction power of ethylene glycol increases with an increase in temperature. At lower temperatures only the covellite phase (CuS) exists but at elevated temperatures CuS decomposed to form chalcocite (Cu_2S) [18]. Keeping these facts in mind CuS-Cu_2S nanoparticle blends have been successfully synthesized (Scheme 1). Photocatalytic activity was performed against different organic dyes such as methylene blue (MB) (Fig. 1a), malachite green (MG) (Fig. 1b), methyl orange (MO) (Fig. 1c), methyl violet (MV) (Fig. 1d) and rhodamine B (RhB) (Fig. 1e). Previously different research groups have performed photo-catalysis under UV lamp or by producing indoor effects of sunlight with the help of lamps exhibiting power equal to sunlight [1]. In our present research an attempt was made to perform photo-catalysis under direct sunlight i.e. in outdoor lightening. This was the first ever attempt to perform photo-catalysis in outdoor lightening with minimum amount of CuS–Cu_2S as a catalyst used.

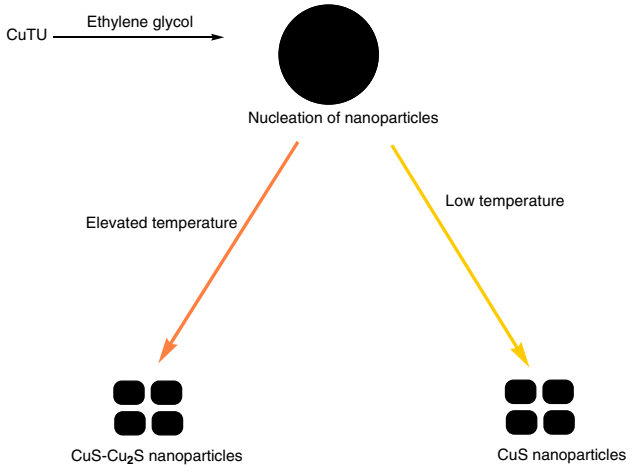

Scheme 1 Schematic illustration for the formation of CuS–Cu2S nanoparticles.

2. Experimental details

2.1. Materials and methods

Gallen-Kemp (U.K) electro thermal melting point apparatus was used to determine melting points in a capillary tube. Infrared spectrum was recorded between 4000 and 400 cm^{-1} on thermo-scientific NICOLET 6700 FTIR. $Si(CH_3)_4$ was used as internal reference to record ^1H and ^{13}C NMR spectra on Joel JNM-LA 500 FT-NMR between 0 and 13 ppm and 0 and 210 ppm respectively. UV–vis absorption spectra were recorded between 200 and 800 nm on Shimadzu 1800 spectrophotometer. CuS–Cu_2S nanoparticles were characterized with Cu Kα radiation of 0.154 nm between diffraction angles of 20–80. Samples were prepared by dispersing them in *n*-Hexane followed by sonication for 10 min. HRTEM of samples was conducted with FEI Company's Titan 80–300 CT transmission electron microscope (TEM) by operating it with acceleration voltage of 300 kV. Moreover, the EDS spectra of samples were also acquired during their conventional transmission electron microscopic (CTEM) investigations. For crystal structure determination the SAED patterns from various regions of samples were acquired. It should be noted that the entire electron micrographs acquired with TEM were recorded on a 4 k × 4 k charge coupled device (CCD) camera of model US4000 from Gatan, Inc.

2.2. Synthesis of 1-(2-chloro-4-nitrophenyl)-3-propionylthiourea (TU)

New thiourea namely 1-(2-chloro-4-nitrophenyl)-3-propionyl thiourea was synthesized by the reaction of propionyl chloride with 2-chloro-4-nitroaniline, in the presence of potassium thiocyanate in two steps. In the 1st step, propionyl chloride was added drop wise to a solution of potassium thiocyanate in dry acetone (1:1). Soon after mixing white precipitates of potassium chloride (formed as a byproduct) appeared, the reaction mixture was kept on stirring for 2 h. In the 2nd step, solution of nitroaniline in dry acetone (again taken in 1:1) was added to the reaction mixture and kept on reflux overnight. The reaction mixture was then transferred to a beaker containing ice to dissolve potassium chloride and stirred for 2 h to settle the TU for precipitation. The precipitates were collected by filtration, washed with distilled water and dried. The prepared

Please cite this article in press as: U. Shamraiz et al., Surfactant free fabrication of copper sulphide (CuS–Cu_2S) nanoparticles from single source precursor for photocatalytic applications, Journal of Saudi Chemical Society (2015), http://dx.doi.org/10.1016/j.jscs.2015.07.005

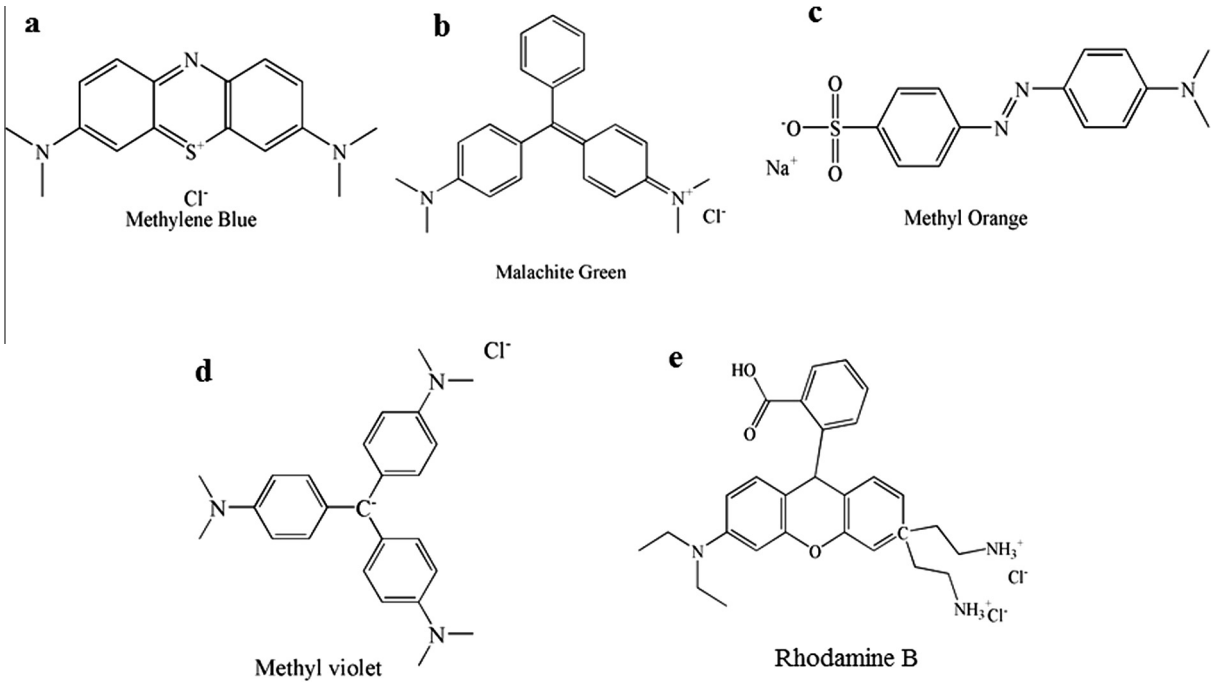

Figure 1 Molecular structures of dyes.

TU was tested, for its solubility in different solvents and was kept for crystallization in acetone [18].

2.2.1. Quantities used

0.5 g (0.0051 mol) of KSCN, 0.42 mL (0.0051 mol) of propionyl chloride, 0.884 g (0.0051 mol) of 2-chloro-4-nitroanaline. Yield (:) 73%; mp 115 °C; H^1 NMR (DMSO) δ (ppm) 12.95 (s, NH), 11.80 (s, NH), ~8.1 (d, J = 72.3 Hz, C3H), ~7.9 (dd, J = 17.4 Hz, C5H), ~6.8 (t, J = 21.9 Hz, C6H), ~2.45 (dd, J = 22.5 Hz, CH2), ~1.1 (t, J = 15.0 Hz, CH3); C^{13} NMR (DMSO) δ (ppm) 176.6 (C═S), 173.73 (C═O), 141.66 (C1), 136.3 (C2), 125.26 (C3), 143.45 (C4), 116.2 (C5), 127.89 (C6), 29.7 (CH2), 9.76 (CH3). FTIR υ_{max} (cm^{-1}) 3285–3210 (NH), 3092 (Ar CH), 1635 (C═O), 1587 (C═S), 1273 (C-N); (Fig. S1).

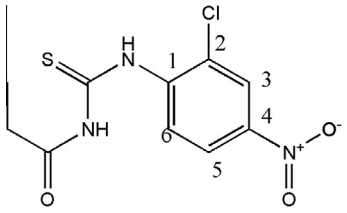

2.3. Synthesis of bis(1-(2-chloro-4-nitrophenyl)-3-propionylthiourea)copper(II) (CuTU)

Copper acetate monohydrate in 20 mL methanol/DCM mixture was added drop wise to the solution of TU synthesized in the 1st step. The solution was then refluxed for about 6 h until the formation of a green coloured product. The resulting mixture was then filtered off and washed several times with methanol and DCM (Scheme 2).

2.3.1. Quantities used

Copper acetate monohydrate 0.0694 g (0.0034 mol); TU2 0.2 g (0.00069 mol). Yield (:) 64%; mp 146 °C; FTIR υ_{max} (cm^{-1}) 3270 (NH), 3092 (Ar CH), 1675 (C═O) 1190 (C–S), 432 (Cu–S) (Fig. S2). The IR data in tabulated form are presented in Table 1.

In FTIR spectra for ligand NH protons are available between 3285 and 3210 cm^{-1} and Aromatic protons appear slightly above 3000 cm^{-1}. The carbonyl appears at 1635 cm^{-1} as an intense peak while thionyl appears at 1587 cm^{-1}. In FTIR spectra the disappearance of one NH peak above 3200 cm^{-1} is a strong evidence for complexation between copper and thiourea ligand. The carbonyl peak is also shifted to a higher wave number and appears as an intense peak at 1675 cm^{-1}, while peak appearing at 1190 cm^{-1} corresponds to C–S and peak at 432 cm^{-1} can be attributed to the formation of Cu–S.

2.4. Fabrication of CuS

CuS–Cu_2S nanoparticles were fabricated in ethylene glycol reducing environment. No surfactant or capping agent was used during the process. The reaction mixture containing 0.8 g of CuTU in 25 mL of ethylene glycol in a two neck round bottom flask was kept under reflux for 8 h at 180 °C. The black precipitates were then collected by dispersing the resulting solution in 300 mL methanol, which were then filtered off, washed several times with deionized water and methanol, and dried in an oven at 70 °C.

2.5. Photocatalytic activity of CuS–Cu_2S

Photocatalytic activity was carried out by considering the stability of organic dyes under various pH conditions and strong absorption in visible region for cationic dyes such as methyl

Please cite this article in press as: U. Shamraiz et al., Surfactant free fabrication of copper sulphide (CuS–Cu_2S) nanoparticles from single source precursor for photocatalytic applications, Journal of Saudi Chemical Society (2015), http://dx.doi.org/10.1016/j.jscs.2015.07.005

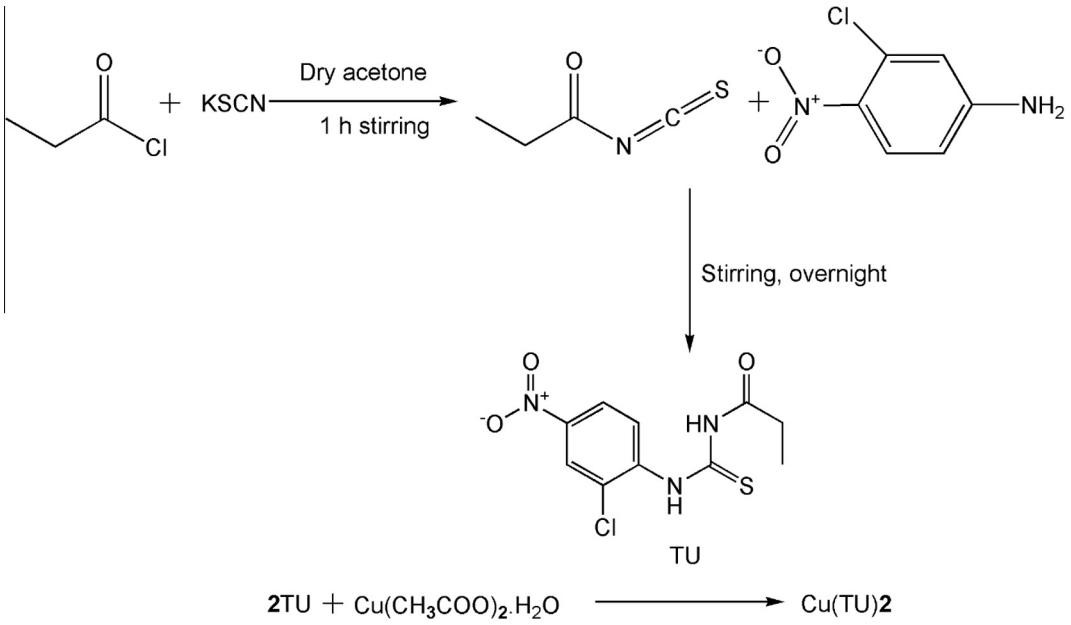

Scheme 2 Synthesis of TU ligand and CuTU complex.

Table 1 IR data of TU and CuTU.

Absorbing groups	TU	CuTU
ν(N–H) cm^{-1}	3285–3210	3270
ν(C–H_{ar}) cm^{-1}	3092	3092
ν(C═O) cm^{-1}	1635	1675
ν(C═S) cm^{-1}	1587	
ν(C–N) cm^{-1}	1273	
ν(C–S) cm^{-1}		1190
ν(Cu–S) cm^{-1}		432
ν(C═N) cm^{-1}		1595

violet (MV), methylene blue (MB), rhodamine B (RhB), malachite green (MG) and anionic dye like methyl orange (MO) [40]. Direct sunlight (outdoor lightening) was used as a source of energy for photo degradation of dyes. Photocatalytic activity for 0.01 g (10 mmol) of CuS–Cu_2S was assessed separately using 25 mL of 10^{-5} M aqueous solution of different dyes. It was observed that except methyl orange, all other organic dyes used in this article for photo catalysis provided a decrease in their λ_{max}. The outdoor sunlight has been shown to be very effective for photo catalysis. Self-degradation of dyes was evaluated by running blank samples under same conditions without catalyst.

3. Results and discussion

Many phases of copper sulphide occur in nature which are stable under normal conditions such as covellite (CuS), anilite ($Cu_{1.75}S$), digenite ($Cu_{1.8}S$), dijuralite ($Cu_{1.96}S$) and chalcocite (Cu_2S) [6]. The phase, purity and polycrystalline nature of the CuS–Cu_2S samples are initially characterized using powder X-ray diffraction (PXRD) measurement. The presence of strong and intense diffraction peaks indicates the preferential growth of atoms along (1 0 1), (1 0 2), (1 0 3), (1 1 0), (1 0 8) and (1 1 6) planes of primitive hexagonal covellite phase [41]. In addition to these peaks an intense peak at 46.74, 2Θ is due to the presence of Cu_2S which is a characteristic peak for Cu_2S [42]. The XRD pattern has been compared with the data from JCPDS Card No. 00-001-1281 and indexed as hexagonal crystal system of CuS with $P63/mmc$ space group and a primitive hexagonal unit cell with $a = 3.8020$ and $c = 16.430$ Å.

3.1. Structural characterization of CuS–Cu_2S

To study the degree of crystallinity and structure of the synthesized CuS–Cu_2S nanoparticles EDX, TEM, HRTEM, and SAED analyses have been performed. CuS–Cu_2S was prepared with an average of 21.5 nm which has been confirmed with Scherrer formulae (Eq. (1)).

$$d = \frac{0.94\lambda}{\mathrm{FWHM}(2\Theta)\mathrm{Cos}\Theta} \quad (1)$$

where "0.94" is a constant, "Θ" is Bragg's angle of the particular peak under consideration and "d" is the crystallite size of the nanoparticles [11]. Phase purity of CuS–Cu_2S has been confirmed by PXRD and all the peaks in powder XRD are indexed for hexagonal crystalline phase of covellite (CuS) with lattices growing mostly in the direction of 110 plane. Along with these peaks some other peaks also appeared in which significant peak at 46.74, 2Θ is due to the presence of the chalcocite (Cu_2S) phase, because at high temperatures the reduction power of ethylene glycol increases and formation of chalcocite becomes favourable. The sharpness of peaks is also an indication of the crystalline nature of the sample (Fig. 2a). Furthermore the purity of the sample was confirmed with EDX recorded on nanostructures which show the elemental composition of CuS–Cu_2S which confirms that sample was enriched with copper and sulphur, without any additional peaks for other elements. Copper Cu Kα and Cu Kβ appear at 8.04 and 8.90 keV which corresponds to X-rays of 1.54 and 1.39 Å and Cu Lα appears at 0.92 keV which corresponds

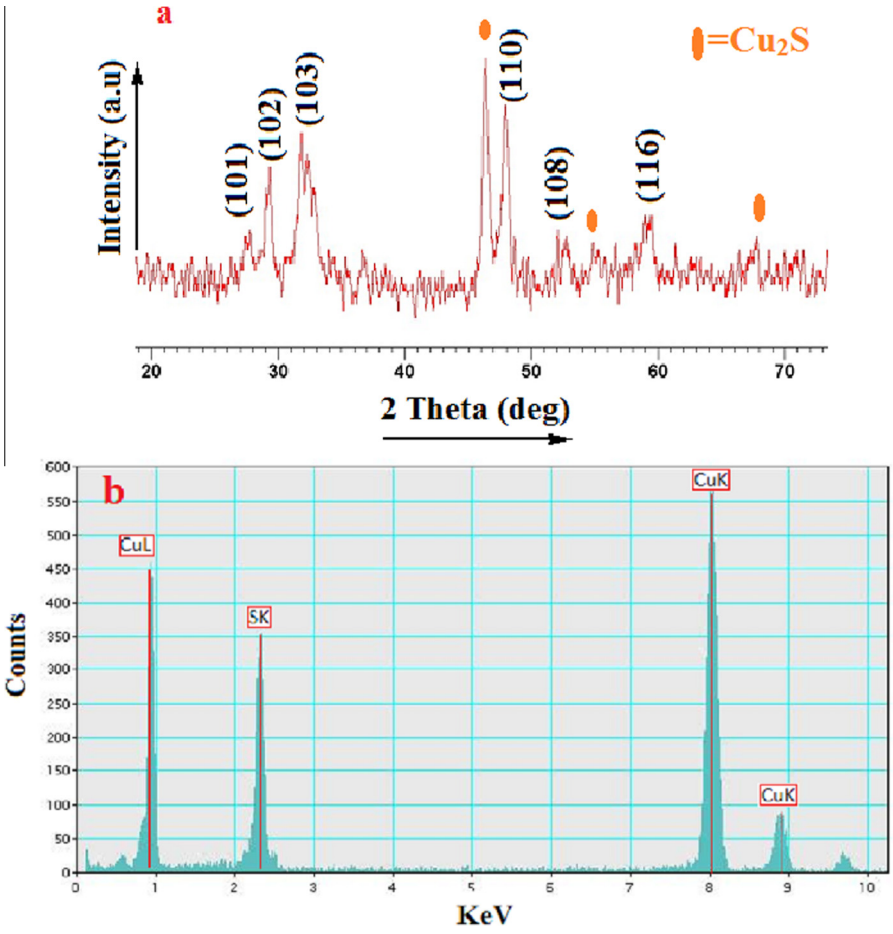

Figure 2 (a) XRD pattern of prepared CuS–Cu_2S nanoparticles in ethylene glycol, (b) EDX image showing only the presence of copper and sulphur in the sample.

to emission of 13.33 Å, while S Kα appears at 2.37 keV due to the emission of X-rays in the region of 5.37 Å (Fig. 2b).

In SAED images, cone formation clearly represents the poly nano-crystalline nature of the sample while each cone presents specific planes that were also present in PXRD, which also confirms the d spacings for specific planes (Fig. 3a). Morphological studies were performed with the help of TEM and HRTEM, interpretation proved that sample was in the form of well dispersed nanoparticles with an average of less than 30 nm in diameter and HRTEM (Fig. 3b–d) images further confirmed, that CuS synthesized was present in the form of nanoparticles and provide lattice fringes for 110 plane having *d* spacing of 1.89 Å, and confirms that most of the particles grow in that specific direction.

3.2. Photo degradation of dye molecules

Photo degradation of dyes depends on adsorption of dye over catalyst which is itself dependent on surface area of catalyst used i.e. the larger the surface area the higher will be the adsorption. The surface area in turn depends on the size of the nanoparticles (the smaller the size the larger is the surface area). Keeping these facts in mind synthesized CuS–Cu_2S were used to monitor photocatalytic activities against five different organic dyes.

Dye solutions in 25 mL volumetric flask, containing 10 mg of the catalyst CuS–Cu_2S were irradiated under direct sunlight (outdoor lightening) to carry out photo degradation of dyes. The photocatalytic activity of CuS–Cu_2S nanoparticles was monitored as a successive decrease in the characteristic absorption peaks with passage of irradiation time for all dyes used. It was observed that the degradation process is quite faster for cationic dyes like methyl violet (MV), methylene blue (MB), malachite green (MG) and rhodamine B (RhB) but quite slow for anionic dyes like methyl orange (MO). The degradation of cationic dyes by CuS–Cu_2S is due to the presence of active negative charges on its surface, which are the active agents for degradation of cationic dyes. The negative charge on the surface is possibly due to surface bound OH^-. Electron transfer under the application of direct sunlight is facilitated by the electrostatic force of attraction between cationic dye molecules and anionic surface of the catalyst which is not possible in case of anionic dyes, but due to large structural spread outs these become slightly polarizable and hence electron transfer is facilitated up to certain extent. Large surface area of catalyst in case of nano photo catalyst is of prime concern for effective degradation, which results in a large number of unsaturated coordination sites to adsorb dye molecules. The OH^- present on the surface of nanoparticles may come from different sources. The possible OH^- sources are (i) transformation of surface bound oxygen that is adsorbed during the process (ii)

Please cite this article in press as: U. Shamraiz et al., Surfactant free fabrication of copper sulphide (CuS–Cu_2S) nanoparticles from single source precursor for photocatalytic applications, Journal of Saudi Chemical Society (2015), http://dx.doi.org/10.1016/j.jscs.2015.07.005

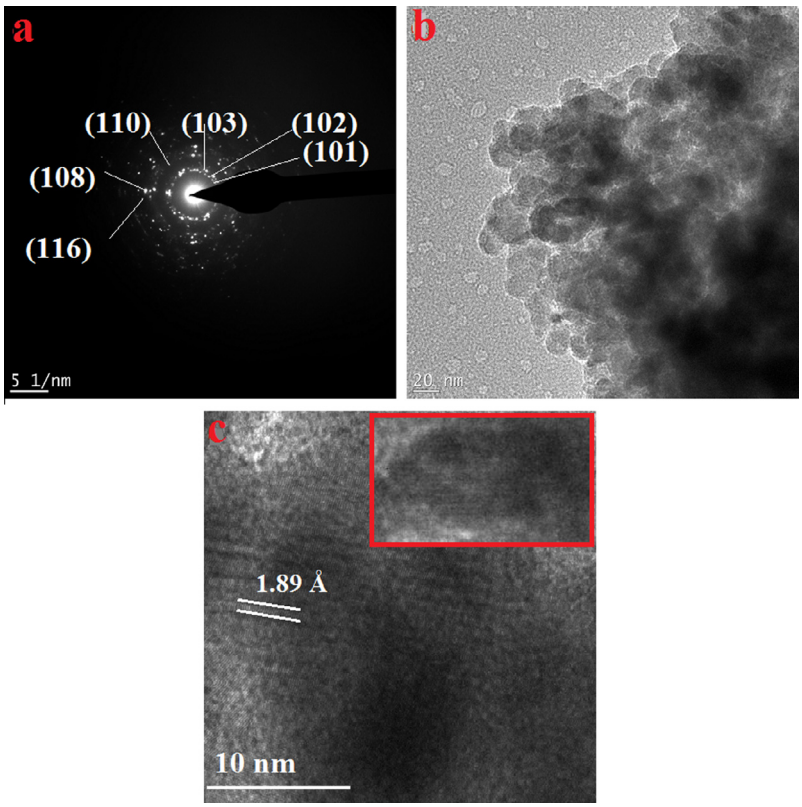

Figure 3 (a) SAED pattern of nanoparticles, (b) TEM image of nanoparticles, (c) HRTEM images of nanoparticle prepared without any surfactant in the presence of ethylene glycol.

oxidation of water molecules released during dissociation of ethylene glycol at reaction temperature. In this way electron transfer in the presence of sunlight (outdoor lightening) is facilitated with reactive oxygen radicals. The OH^- radicals and photo produced holes are two possible active oxidative agents that take part in photocatalytic reactions [43].

3.3. Mechanism of dye degradation

Solar light was used as energy source, because it has sufficient energy to eject electrons from the valence shell of photo catalyst and then create electron/hole pairs in the photo catalyst which are necessary to react with dissolved oxygen molecules in the sample to form O_2^- and holes then generate OH°, which then act as active centre to react with organic dyes to oxidize them (Fig. 4). The dye molecules contain double bonds which are susceptible to attack by the so formed free radicals on the surface of the catalyst. When these double bonds are exposed to free radicals they react with free radicals and the electron is transferred via free radical to double bond of the dye molecule and dissociation of dye molecule occurs, which are converted into byproducts and hence, degradation of dyes occurs efficiently. Self-degradation of dyes was further evaluated by running blank samples without catalyst under same conditions. It was observed that except malachite green all other dyes used for degradation were quite stable towards direct sunlight. It can be generalized that electron transfer is facilitated from catalyst to dyes by the generation of electron-hole pair under the application of direct sunlight, and in addition to this dye adsorption is necessary for electron transfer otherwise no degradation occurs.

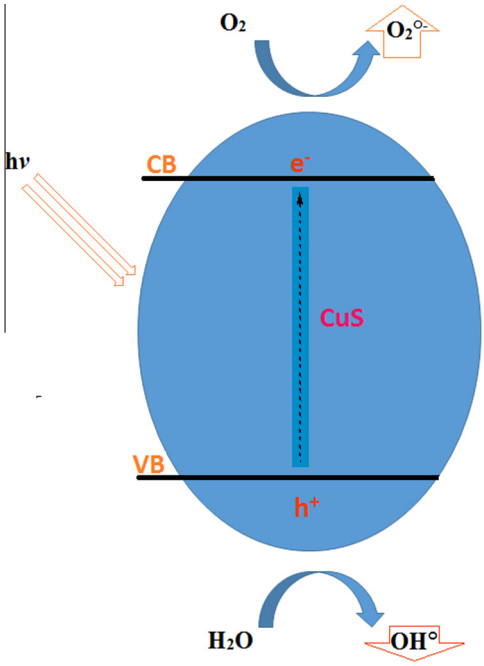

Figure 4 Schematic dye degradation by CuS–Cu_2S nano-photocatalyst.

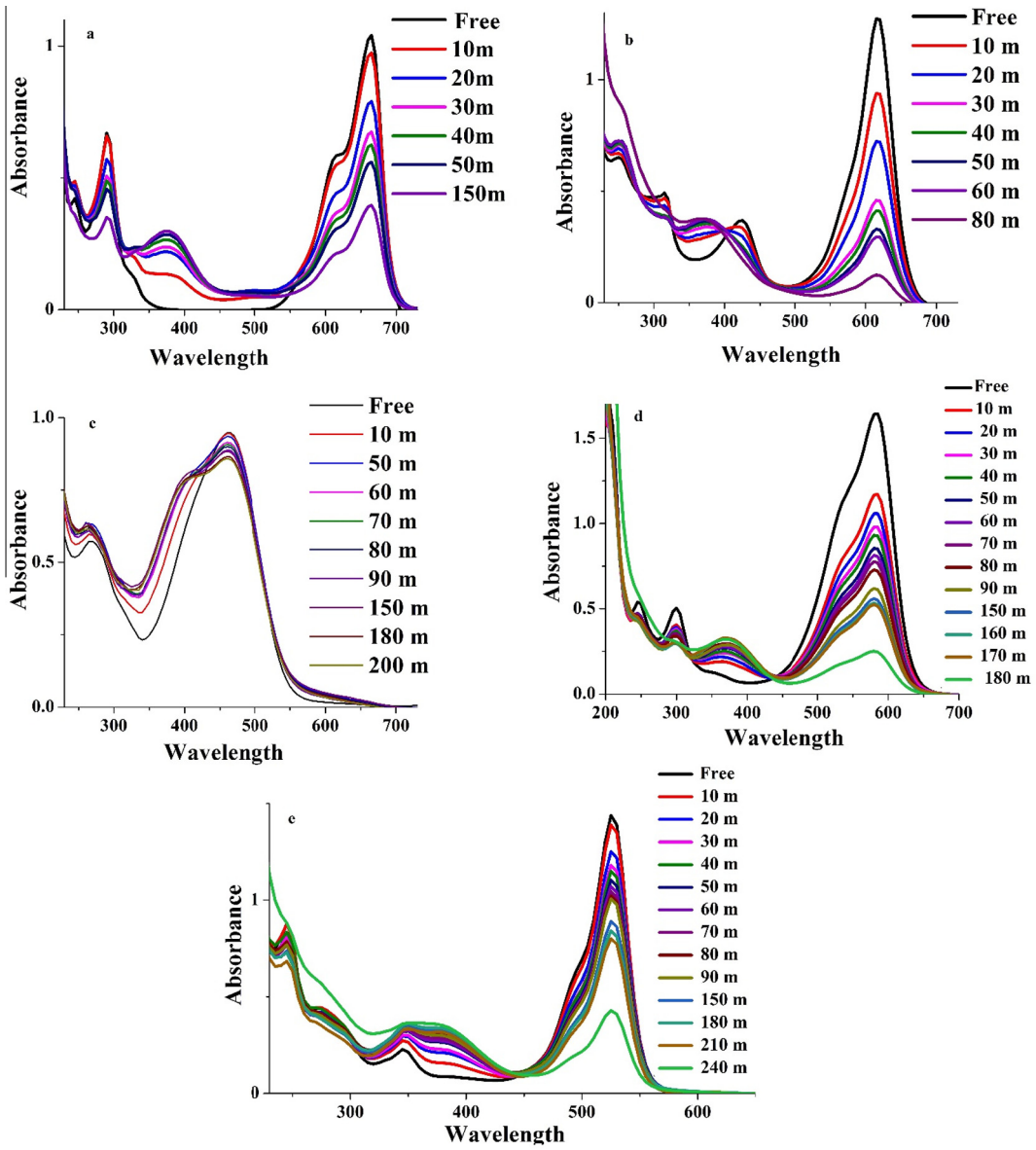

Figure 5 UV–visible absorption spectra at different durations with the addition of 10 mg of CuS–Cu_2S and irradiated under direct sunlight (outdoor lightening), (a) methylene blue, (b) malachite green, (c) methyl orange, (d) methyl violet, (e) rhodamine B.

The characteristic absorption peaks of all the dye molecules were used to monitor the degradation of dyes with the passage of irradiation time. Successive decrease in peak intensity with irradiation time indicates the degradation of dye molecules. Dye degradation was evaluated with the help of following equation:

$$(1 - A_t/A_o) \times 100 \quad (2)$$

where A_o is the initial absorbance and A_t is the absorbance at the time t [18].

In case of methylene blue (MB) which is a cationic dye the intense peak at 665 nm was used to evaluate the overall activity. Almost 50% degradation was achieved in the first 20 min, because initially more active coordination sites are available for adsorption of dye molecules while after 100 min, overall 61.95% of dye degradation was achieved (Fig. 5a).

Whereas, in case of malachite green (MG, again a cationic dye) the peak chosen to monitor photocatalytic activity was at 615 nm. It was further observed that MG is unstable under the application of direct sunlight. To eliminate its self-degradation a blank sample without catalyst was also run under same conditions. After 40 min of exposure time 90.25% of dye molecules were degraded with catalyst while without catalyst the degradation was only 61%. This clearly indicates, that the catalyst used was active under the application of direct sunlight and degraded dye molecules efficiently (Fig. 5b).

In case of MO which is an anionic dye the intense peak at 455 nm was used to observe the overall degradation efficiency. Only 9.39% of dye degradation was observed with the irradiation time of 180 min. In addition to this it was further observed that in case of methyl orange a blue shift was observed in the characteristic absorption peak or a shoulder

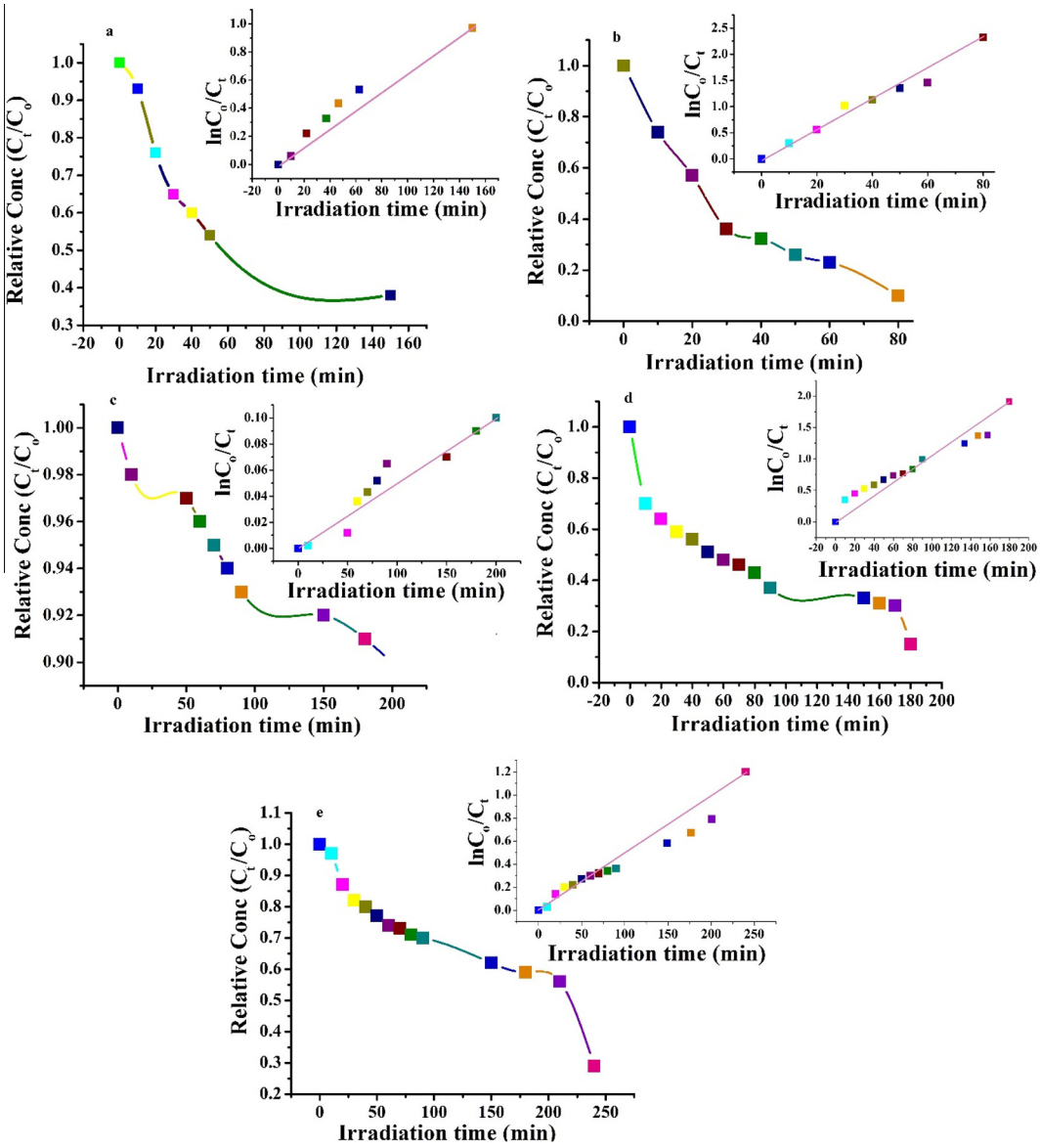

Figure 6 Photocatalytic degradation following pseudo-first order kinetics of (a) methylene blue, (b) malachite green, (c) methyl orange, (d) methyl violet, (e) rhodamine B.

Table 2 Comparison of the rate constants for CuS–Cu_2S.

Dyes	Rate constant (min^{-1}) CuS–Cu_2S
MB	6.40×10^{-3}
MG	2.95×10^{-2}
MO	4.93×10^{-4}
MV	1.06×10^{-2}
RhB	5.0×10^{-2}

appears with blue shift along with the characteristic absorption peak. This might be due to demethylation of MO, which are most probably replaced with H atoms [44] (Fig. 5c).

MV also known as crystal violet is a cationic dye and provides an intense peak at 585 nm which was used to evaluate the photo catalysis under outdoor lightening. Almost 50% of dye degradation was achieved in 10 min after exposing under sunlight while 85.03% of dye molecules were degraded when sample was exposed to sunlight for 60 min (Fig. 5d).

Rhodamine B (RhB) is another dye mostly used as a tracer to determine rate and direction of flow in water, possesses active positive nitrogen centre, provides intense peak at 525 nm which was used to carryout degradation of the dye. 70.16% of the dye molecules were degraded with the exposure time of 80 min under direct sunlight (Fig. 5e).

3.4. Kinetics of dye degradation

Degradation of dyes with CuS–Cu_2S was studied by monitoring successive decrease in the characteristic absorption peaks for different dyes. The time dependent relative concentration changes of dyes with CuS–Cu_2S (Fig. 6) are compared. The degradation plots specify that the kinetics of reaction is considered to be the pseudo first order reaction whose kinetics can be expressed by the equation:

$$A = \varepsilon CL \quad (3)$$

$$C = A/\varepsilon L \quad (4)$$

where ε is the molar extinction coefficient which depends on the kind of material used, and L is the path length of the cell used for UV measurements [45].

$$\ln(C_o/C_t) = kt \quad (5)$$

$$K = \ln(C_o/C_t)/t \quad (6)$$

where C_o represents the initial concentration, C_t denotes the concentration at a given time and k is the reaction rate constant [46]. From the given equation reaction rate constants have been obtained and are listed in Table 2.

4. Conclusion

CuS–Cu_2S nanoparticles without any surfactant at moderate temperature with average size of less than 30 nm have been successfully fabricated from copper thiourea complex. We have demonstrated after complete characterization of CuS–Cu_2S nanoparticles the synthesized nanoparticles are active photo catalyst for dye degradation under the application of direct sunlight (outdoor lightening). Dye degradation efficiency was more than 70% for malachite green, methyl violet and rhodamine B. We conclude that except malachite green all other dyes were stable towards sunlight. Dye degradation was negligible for methyl orange. We propose that this difference is due to the interaction of the cationic dye molecules with negatively charged surfaces of CuS–Cu_2S nanoparticles however methyl orange being an anionic dye cannot behave in the same way.

Acknowledgements

We are thankful to the Higher Education Commission, Islamabad, Pakistan for financial assistance.

Appendix A. Supplementary data

Supplementary data associated with this article can be found, in the online version, at http://dx.doi.org/10.1016/j.jscs.2015.07.005.

References

[1] P.K. Bajpai, S. Yadav, A. Tiwari, H.S. Virk, Solid State Phenom. Trans. Tech Publ. (2015) 187–233.
[2] C. Wu, S.-H. Yu, S. Chen, G. Liu, B. Liu, J. Mater. Chem. 16 (2006) 3326–3331.
[3] P. Roy, S.K. Srivastava, Cryst. Growth Des. 6 (2006) 1921–1926.
[4] H. Wu, W. Chen, Nanoscale 3 (2011) 5096–5102.
[5] P. Roy, K. Mondal, S.K. Srivastava, Cryst. Growth Des. 8 (2008) 1530–1534.
[6] Z. Cheng, S. Wang, Q. Wang, B. Geng, CrystEngComm 12 (2010) 144–149.
[7] G. Ku, M. Zhou, S. Song, Q. Huang, J. Hazle, C. Li, ACS Nano 6 (2012) 7489–7496.
[8] S. Sun, X. Song, C. Kong, D. Deng, Z. Yang, CrystEngComm 14 (2011) 67–70.
[9] X. Chen, Z. Wang, X. Wang, R. Zhang, X. Liu, W. Lin, Y. Qian, J. Cryst. Growth 263 (2004) 570–574.
[10] J.P. Gramp, K. Sasaki, J.M. Bigham, O.V. Karnachuk, O.H. Tuovinen, Geomicrobiol. J. 23 (2006) 613–619.
[11] A. Ubale, D. Choudhari, J. Kantale, V. Mitkari, M. Nikam, W. Gawande, P. Patil, J. Alloys Compd. 509 (2011) 9249–9254.
[12] L. Reijnen, B. Meester, F. de Lange, J. Schoonman, A. Goossens, Chem. Mater. 17 (2005) 2724–2728.
[13] K.-J. Wang, G.-D. Li, J.-X. Li, Q. Wang, J.-S. Chen, Cryst. Growth Des. 7 (2007) 2265–2267.
[14] J. Xu, X. Cui, J. Zhang, H. Liang, H. Wang, J. Li, Bull. Mater. Sci. 31 (2008) 189–192.
[15] H. Wang, J.-R. Zhang, X.-N. Zhao, S. Xu, J.-J. Zhu, Mater. Lett. 55 (2002) 253–258.
[16] W. Wang, L. Ao, Mater. Chem. Phys. 109 (2008) 77–81.
[17] C. Chen, Q. Li, Y. Wang, Y. Li, X. Zhong, Front. Optoelectron China 4 (2011) 150–155.
[18] M. Basu, A.K. Sinha, M. Pradhan, S. Sarkar, Y. Negishi, T. Pal, Environ. Sci. Technol. 44 (2010) 6313–6318.
[19] A. Muszer, J. Wódka, T. Chmielewski, S. Matuska, Hydrometallurgy 137 (2013) 1–7.
[20] X. Dong, D. Potter, C. Erkey, Ind. Eng. Chem. 41 (2002) 4489–4493.
[21] J. Mao, Q. Shu, Y. Wen, H. Yuan, D. Xiao, M.M. Choi, Cryst. Growth Des. 9 (2009) 2546–2548.
[22] R. Mane, C. Lokhande, Mater. Chem. Phys. 65 (2000) 1–31.
[23] S. He, G.S. Wang, C. Lu, X. Luo, B. Wen, L. Guo, M.S. Cao, ChemPlusChem 78 (2013) 250–258.
[24] J.-S. Chung, H.-J. Sohn, J. Power Sources 108 (2002) 226–231.
[25] J. Xu, J. Zhang, C. Yao, H. Dong, J. Chilean Chem. Soc. 58 (2013) 1722–1724.
[26] S. Gorai, D. Ganguli, S. Chaudhuri, Mater. Chem. Phys. 88 (2004) 383–387.
[27] H.-T. Zhang, G. Wu, X.-H. Chen, Langmuir 21 (2005) 4281–4282.
[28] Z. Li, W. Chen, H. Wang, Q. Ding, H. Hou, J. Zhang, L. Mi, Z. Zheng, Mater. Lett. 65 (2011) 1785–1787.
[29] M. Peng, L.-L. Ma, Y.-G. Zhang, M. Tan, J.-B. Wang, Y. Yu, Mater. Res. Bull. 44 (2009) 1834–1841.
[30] H. Lee, S.W. Yoon, E.J. Kim, J. Park, Nano Lett. 7 (2007) 778–784.
[31] S. Lv, H. Suo, X. Zhao, C. Wang, T. Zhou, S. Jing, Y. Xu, C. Zhao, J. Alloys Compd. 479 (2009) L43–L46.
[32] M. Mousavi-Kamazani, M. Salavati-Niasari, Composites Part B: Engineering, 56 (2014) 490–496.
[33] X. Yu, X. An, Mater. Lett. 64 (2010) 252–254.
[34] S. Gorai, D. Ganguli, S. Chaudhuri, Mater. Lett. 59 (2005) 826–828.
[35] Y. Zhu, D. Fan, W. Shen, Langmuir 24 (2008) 11131–11136.
[36] L. Reijnen, B. Meester, F. de Lange, J. Schoonman, A. Goossens, Chem. Mater. 17 (2005) 2724–2728.
[37] D. Mohan, C.U. Pittman Jr, J. Hazard. Mater. 142 (2007) 1–53.
[38] A. Phuruangrat, T. Thongtem, S. Thongtem, Chalco. Lett. 8 (2011) 291–295.
[39] H.Y. He, Int. J. Environ. Res. 2 (1) (2008) 23–26.
[40] M.K. Rauf, A. Badshah, M. Gielen, M. Ebihara, D. de Vos, S. Ahmed, J. Inorg. Biochem. 103 (2009) 1135–1144.
[41] Y.-B. Chen, L. Chen, L.-M. Wu, Cryst. Growth Des. 8 (2008) 2736–2740.
[42] Y. Zhu, X. Guo, J. Jin, Y. Shen, X. Guo, W. Ding, J. Mater. Sci. 42 (2007) 1042–1045.
[43] A. Sobhani, M. Salavati-Niasari, S.M. Hosseinpour-Mashkani, J. Cluster. Sci. 23 (2012) 1143–1151.
[44] G. Lin, J. Zheng, R. Xu, J. Phys. Chem. C 112 (2008) 7363–7370.
[45] K. Fuwa, B. Valle, Anal. Chem. 35 (1963) 942–946.